Modeling and Analysis of Dual-Stator Windings Self-Excited Induction Generator

Hocine Amimeur, Rachid Abdessemed, Djamal Aouzellag, Elkhier Merabet and Farid Hamoudi

***Abstract*— This paper presents a detailed modeling and the analysis of a dual-stator windings self-excited induction generator. The mathematical model has been developed in synchronous reference frame; in this one, the effects of the common mutual leakage inductance between the two three-phase windings sets have been included. Dynamics of self-excitation process, and step application of load are simulated.**

***Index Terms*— Analysis, dual-stator windings induction generator, modeling, self-excited.**

I. Introduction

ENVIRONMENTAL concerns international policies are supporting new interests and developments in small-scale power generation during the last few years [1]. Therefore, the study of self-excited induction generator has regained importance, as they are particularly suitable for wind and small hydro power plants [2]. The primary advantages of self-excited induction generator are less maintenance cost, better transient performance, without dc power supply for field excitation, brushless construction (squirrel-cage rotor), etc. [3].

Since the late 1920s, dual-stator ac applications, for their advantages in power segmentation, reliability, lower torque pulsations, less dc-link current harmonics, reduced rotor harmonics currents and higher power per ampere ratio for the same machine volume, etc. [4]-[6].

The excitation can be provided by a capacitor bank to the stator windings of the induction generator [7]. Magnetizing inductance is the main factor for voltage buildup and stabilization of generated voltage for the unloaded and load conditions of the induction generator [8].

The terminal capacitor is such a machine must have certain minimum and maximum value for self excitation to take place. This value is affected by machine parameters, speed and load conditions [9].

While being based on the theoretical and experimental works done by the Ref. [14] in which the evolution of the magnetization current is not represented, this article comes to reinforce the results gotten previously by the reference quoted and to bring the thinning on the evolution of the magnetization current seen its fundamental importance.

H. Amimeur, R. Abdessemed, E. Merabet and F. Hamoudi are with the group LEB-Research Laboratory, Department of Electrical Engineering, University of Batna. Street Chahid Mohamed El hadi Boukhlouf, 05000, Batna, Algeria (e-mail: amimeurhocine2002@yahoo.fr; r.abdessemed@lycos.com; merabet_elkheir@yahoo.fr; f_hamoudi@yahoo.fr).

D. Aouzellag was with Electrical Engineering Department, A. Mira University, Bejaia, Algeria (e-mail: aouzellag@hotmail.com).

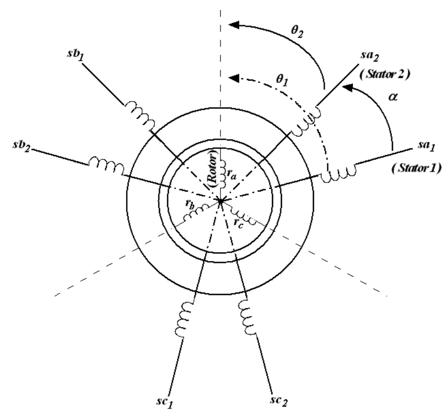

Fig. 1. Dual-stator windings induction machine.

This paper presents a detailed modeling and the analysis of a dual-stator windings induction generator. Dynamics of self-excitation process, and step application of load are simulated.

II. Mathematical Modeling

A schematic of the stator and rotor windings for a dual-stator windings induction machine is given in Fig. 1 [10]. The six stator phases are divided into two wye-connected three-phase sets, labled (sa_1, sb_1, sc_1) and (sa_2, sb_2, sc_2), whose magnetic axes are displaced by an arbitrary angle α. The windings of each three-phase set are uniformly distributed and have axes that are displaced 120 apart. The three-phase rotor windings (r_a, r_b, r_c) are also sinusoidally distributed and have axes that are displaced by 120 apart [12], [15].

Fig. 2 shows the $d-q$ axis equivalent circuit of the dual-stator windings induction machine in the synchronous reference frame.

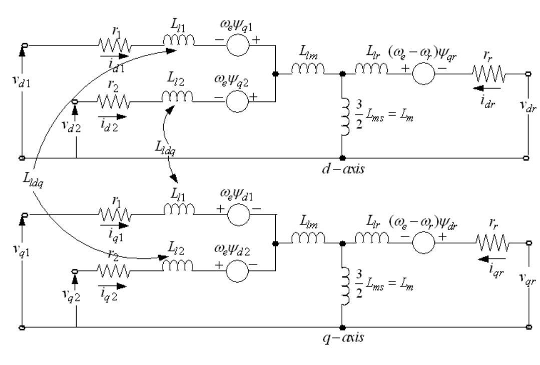

Fig. 2. Equivalent circuit of the dual-stator windings induction machine in the synchronous reference frame.

A. Modeling of the Dual-Stator Windings Induction Generator

The electrical equations of the dual-stator windings induction generator in the synchronous reference frame $(d-q)$ are given as [11]-[12]:

$$v_{d1} = -r_1 i_{d1} - w_e \psi_{q1} + p\psi_{d1} \quad (1)$$

$$v_{q1} = -r_1 i_{q1} + w_e \psi_{d1} + p\psi_{q1} \quad (2)$$

$$v_{d2} = -r_2 i_{d2} - w_e \psi_{q2} + p\psi_{d2} \quad (3)$$

$$v_{q2} = -r_2 i_{q2} + w_e \psi_{d2} + p\psi_{q2} \quad (4)$$

$$v_{dr} = 0 = r_r i_{dr} - (w_e - w_r)\psi_{qr} + p\psi_{dr} \quad (5)$$

$$v_{qr} = 0 = r_r i_{qr} + (w_e - w_r)\psi_{dr} + p\psi_{qr} \quad (6)$$

v_{d1}, v_{d2}, i_{d1}, i_{d2}, and ψ_{d1}, ψ_{d2} are respectively the "d" components of the stator voltages, currents and flux linkage;
v_{q1}, v_{q2}, i_{q1}, i_{q2}, and ψ_{q1}, ψ_{q2} are respectively the "q" components of the stator voltages, currents and flux linkage;
v_{dr}, i_{dr} and ψ_{dr} are respectively the "d" components of the rotor voltage, current and flux linkage;
v_{qr}, i_{qr} and ψ_{qr} are respectively the "q" components of the rotor voltage, current and flux linkage;
r_1, r_2 and r_r are respectively the per phase stator resistance and the per phase rotor resistance;
ω_e is the speed of the synchronous reference frame;
ω_r is the rotor electrical angular speed;
p denotes differentiation $w.r.t$ time [11]-[13].

The expressions for stator and rotor flux linkages are [14]:

$$\psi_{d1} = -L_{l1} i_{d1} - L_{lm}(i_{d1} + i_{d2}) - L_{dq} i_{q2} + L_{md}(-i_{d1} - i_{d2} + i_{dr}) \quad (7)$$

$$\psi_{q1} = -L_{l1} i_{q1} - L_{lm}(i_{q1} + i_{q2}) + L_{dq} i_{d2} + L_{mq}(-i_{q1} - i_{q2} + i_{qr}) \quad (8)$$

$$\psi_{d2} = -L_{l2} i_{d2} - L_{lm}(i_{d1} + i_{d2}) + L_{dq} i_{q1} + L_{md}(-i_{d1} - i_{d2} + i_{dr}) \quad (9)$$

$$\psi_{q2} = -L_{l2} i_{q2} - L_{lm}(i_{q1} + i_{q2}) - L_{dq} i_{d1} + L_{mq}(-i_{q1} - i_{q2} + i_{qr}) \quad (10)$$

$$\psi_{dr} = L_{lr} i_{dr} + L_{md}(-i_{d1} - i_{d2} + i_{dr}) \quad (11)$$

$$\psi_{qr} = L_{lr} i_{qr} + L_{mq}(-i_{q1} - i_{q2} + i_{qr}) \quad (12)$$

The saturation-dependent coefficients of fully saturated induction machine are evaluated [14], [17]-[19] as

$$L_{md} = L_m + \frac{i_{md}}{i_{mq}} L_{dq} = L\cos^2\mu + L_m \sin^2\mu \quad (13)$$

$$L_{mq} = L_m + \frac{i_{mq}}{i_{md}} L_{dq} = L\sin^2\mu + L_m \cos^2\mu \quad (14)$$

$\cos\mu = i_{md}/|\overline{i_m}|$ and $\sin\mu = i_{mq}/|\overline{i_m}|$.

$$L_{s1d} = L_{l1} + L_{md} \quad (15)$$

$$L_{s1q} = L_{l1} + L_{mq} \quad (16)$$

$$L_{s2d} = L_{l2} + L_{md} \quad (17)$$

$$L_{s2q} = L_{l2} + L_{mq} \quad (18)$$

$$L_{rd} = L_{lr} + L_{md} \quad (19)$$

$$L_{rq} = L_{lr} + L_{mq} \quad (20)$$

where, L_{md} and L_{mq} are respectively the direct and quadrature magnetizing inductance;
L_{s1d}, L_{s1q}, L_{s2d}, L_{s2q}, L_{rd} and L_{rq} are respectively the direct and quadrature of the total stator and rotor inductances;
μ is the angular displacement of magnetizing current space vector with respect to the quadrature axis;
i_{md} and i_{mq} are respectively the direct and quadrature components of the magnetizing current space vector;
L_{dq} is the cross-saturation coupling all axes in space quadrature and is solely due to saturation [14], [17],

$$L_{dq} = \frac{i_{md} i_{mq}}{|\overline{i_m}|} \frac{dL_m}{d|\overline{i_m}|} = \frac{i_{md} i_{mq}}{|\overline{i_m}|^2}(L - L_m) \quad (21)$$

L is the dynamic inductance,

$$L = \frac{d|\overline{\psi_m}|}{d|\overline{i_m}|} \quad (22)$$

i_m and ψ_m are respectively the magnetizing current and the magnetizing flux linkage;
L_m is the magnetizing inductance [18],

$$L_m = \frac{|\overline{\psi_m}|}{|\overline{i_m}|} \quad (23)$$

The relationship between magnetizing inductance (L_m) and magnetizing current (i_m) for induction machine was obtained experimentally [20]-[21], [23]. In Fig. 3 the saturated inductance (L_m) and the dynamic inductance (L) have been plotted against the magnitude of the magnetizing current $|i_m|$.

The magnitude of the magnetizing current $|i_m|$ is calculated as

$$i_m = \sqrt{(-i_{d1} - i_{d2} + i_{dr})^2 + (-i_{q1} - i_{q2} + i_{qr})^2} \quad (24)$$

It follows from (13)-(21) that under linear magnetic conditions $L_{md} = L_{mq} = L_m$, $L_{dq} = 0$, $L_{s1d} = L_{s1q}$, $L_{s2d} = L_{s2q}$ and $L_{rd} = L_{rq}$ [14], [18].

A general mathematical model of the dual-stator windings induction generator can be established as follows:

$$[B][u] = [A][i] + [L]p[i] \quad (25)$$

where, in these equation, $[u]$ and $[i]$ represents 6×1 column matrices of voltage and current [16]:
$[u] = [v_{d1} \quad v_{q1} \quad v_{d2} \quad v_{q2} \quad v_{dr} \quad v_{qr}]^T$,
$[i] = [i_{d1} \quad i_{q1} \quad i_{d2} \quad i_{q2} \quad i_{dr} \quad i_{qr}]^T$,
$[B]$ is defined as
$[B] = diag[1 \quad 1 \quad 1 \quad 1 \quad 0 \quad 0]$.
$[A]$ and $[L]$ are respectively given by matrices (26) and (27),

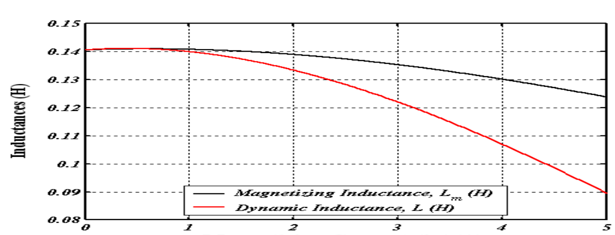

Fig. 3. Variation of the saturated magnetizing inductance and the dynamic inductance with the magnetizing current.

$$[A] = \begin{bmatrix} -r_1 & \omega_e(L_{l1}+L_{lq}) & -\omega_e L_{dq} & \omega_e L_{lq} & 0 & -\omega_e L_{mq} \\ -\omega_e(L_{l1}+L_{ld}) & -r_1 & -\omega_e L_{ld} & -\omega_e L_{dq} & \omega_e L_{md} & 0 \\ \omega_e L_{dq} & \omega_e L_{lq} & -r_2 & \omega_e(L_{l2}+L_{lq}) & 0 & -\omega_e L_{mq} \\ -\omega_e L_{ld} & \omega_e L_{dq} & -\omega_e(L_{l2}+L_{ld}) & -r_2 & \omega_e L_{md} & 0 \\ 0 & \omega_{sl} L_{mq} & 0 & \omega_{sl} L_{mq} & r_r & \omega_{sl}(L_{lr}+L_{mq}) \\ -\omega_{sl} L_{md} & 0 & -\omega_{sl} L_{md} & 0 & \omega_{sl}(L_{lr}+L_{md}) & r_r \end{bmatrix} \quad (26)$$

$$[L] = \begin{bmatrix} -(L_{l1}+L_{ld}) & 0 & -L_{ld} & -L_{dq} & L_{md} & 0 \\ 0 & -(L_{l1}+L_{lq}) & L_{dq} & -L_{lq} & 0 & L_{mq} \\ -L_{ld} & L_{dq} & -(L_{l2}+L_{ld}) & 0 & L_{md} & 0 \\ -L_{dq} & -L_{lq} & 0 & -(L_{l2}+L_{lq}) & 0 & L_{mq} \\ -L_{md} & 0 & -L_{md} & 0 & L_{lr}+L_{md} & 0 \\ 0 & -L_{mq} & 0 & -L_{mq} & 0 & L_{lr}+L_{mq} \end{bmatrix} \quad (27)$$

where L_{ld}, L_{lq} and ω_{sl} are defined as :
$L_{ld} = L_{lm} + L_{md}$, $L_{lq} = L_{lm} + L_{mq}$ and $\omega_{sl} = \omega_e - \omega_r$.

The electromagnetic torque is evaluated as [12], [22]

$$T_{em} = \frac{3}{2}\frac{P}{2}\frac{L_m}{L_r}[(i_{q1}+i_{q2})\psi_{dr} - (i_{d1}+i_{d2})\psi_{qr}] \quad (28)$$

where, $L_r = L_{lr} + L_m$.
The rotor dynamics equation is evaluated as [12], [14]

$$\frac{\omega_r}{\omega_e} = \frac{1}{p}[\frac{1}{\omega_e}\frac{P}{2}\frac{1}{J}(T_{em} - T_{sh})] \quad (29)$$

where T_{sh} is shaft torque, J is moment of inertia and P is number of poles in machine.

B. Modeling of Excitation System

The voltage and current relationship for the excitation capacitance of the dual-stator windings induction generator in the synchronous reference frame $(d-q)$ are given by:

$$pv_{d1} = (i_{d1sh}/C_{sh1}) + w_e v_{q1} \quad (30)$$
$$pv_{q1} = (i_{q1sh}/C_{sh1}) - w_e v_{d1} \quad (31)$$
$$pv_{d2} = (i_{d2sh}/C_{sh2}) + w_e v_{q2} \quad (32)$$
$$pv_{q2} = (i_{q2sh}/C_{sh2}) - w_e v_{d2} \quad (33)$$

where, C_{sh1} and C_{sh2} are respectively the excitation capacitance connected the dual stator windings set I and II;
i_{d1sh} and i_{d2sh} are respectively the "d" components of the currents flowing into excitation capacitor;
i_{q1sh} and i_{q2sh} are respectively the "q" components of the currents flowing into excitation capacitor.

C. Load Model

1) Resistive Load Model : General resistive load is represented in the synchronous reference frame as the generator with the following equations [12], [14]:

$$pv_{d1} = (1/C_{sh1})\{i_{d1} - (v_{d1}/R_1)\} + w_e v_{q1} \quad (34)$$
$$pv_{q1} = (1/C_{sh1})\{i_{q1} - (v_{q1}/R_1)\} - w_e v_{d1} \quad (35)$$
$$pv_{d2} = (1/C_{sh2})\{i_{d2} - (v_{d2}/R_2)\} + w_e v_{q2} \quad (36)$$
$$pv_{q2} = (1/C_{sh2})\{i_{q2} - (v_{q2}/R_2)\} - w_e v_{d2} \quad (37)$$

where, R_1 and R_2 are respectively the load resistances connected across the windings set I and II.

2) Resistive-Inductive Load Model : General resistive-inductive passive load is represented in the synchronous reference frame as the generator with the following equations [12], [19]:

$$\begin{cases} pv_{d1} = (1/C_{sh1})(i_{d1} - i_{d1L}) + w_e v_{q1} \\ pi_{d1L} = (1/L_1)(v_{d1} - R_1 i_{d1L} + w_e L_1 i_{q1L}) \end{cases} \quad (38)$$

$$\begin{cases} pv_{q1} = (1/C_{sh1})(i_{q1} - i_{q1L}) - w_e v_{d1} \\ pi_{q1L} = (1/L_1)(v_{q1} - R_1 i_{q1L} - w_e L_1 i_{d1L}) \end{cases} \quad (39)$$

$$\begin{cases} pv_{d2} = (1/C_{sh2})(i_{d2} - i_{d2L}) + w_e v_{q2} \\ pi_{d2L} = (1/L_2)(v_{d2} - R_2 i_{d2L} + w_e L_2 i_{q2L}) \end{cases} \quad (40)$$

$$\begin{cases} pv_{q2} = (1/C_{sh2})(i_{q2} - i_{q2L}) - w_e v_{d2} \\ pi_{q2L} = (1/L_2)(v_{q2} - R_2 i_{q2L} - w_e L_2 i_{d2L}) \end{cases} \quad (41)$$

where, L_1 and L_2 are respectively the load inductances connected across the windings set I and II;
i_{d1L}, i_{d2L} and i_{q1L}, i_{q2L} are respectively the "d" and "q" components of the load current.

III. Simulation Results and Discussion

The simulation in this paper has been developed in MATLAB/SIMULINK® environment. In the model the prime mover speed (ω_r) and the excitation capacitance are fixed at $314.5 rad/s$, and $C_{sh1} = C_{sh2} = 40\mu F/phase$ respectively. The dual-stator windings induction machine parameters used in the simulation are given in the Appendix.

A. Excitation with no Load

Figs. 4 and 5 show respectively the stator voltages and currents variations (winding set I and II) at no load conditions of the dual-stator winding induction generator. At the start-up the voltages and the currents generated by the sets I and II increase in exponential form, then they stabilize respectively at $224V$ and $2.85A$ at time $2.25s$ and it is the moment when the magnetizing current reach his so saturated regime (Fig. 6) approximatively at $6.9A$. We observe that the variation of voltages and stator currents follow the variation of the magnetizing current.

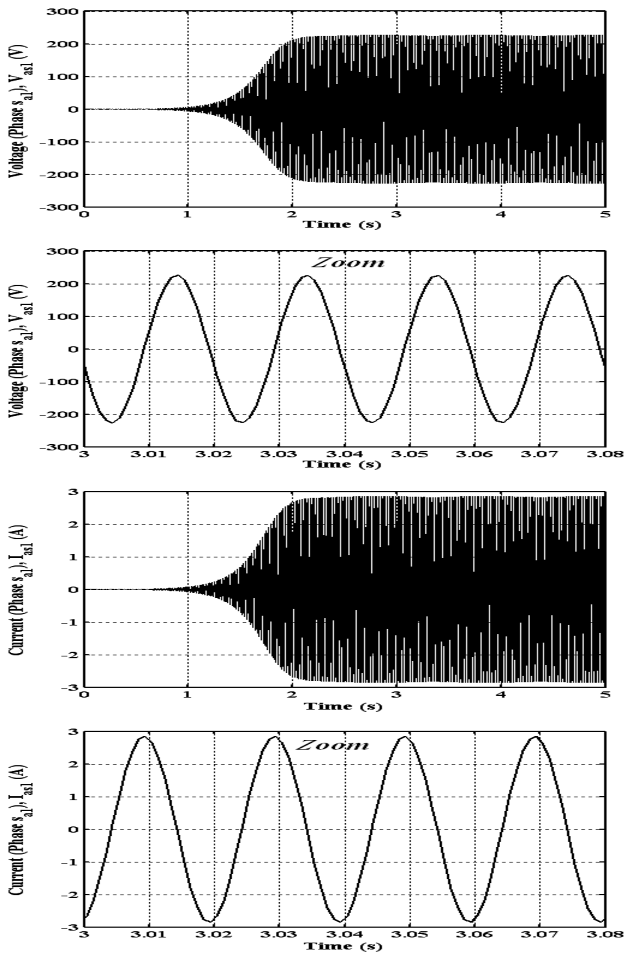

Fig. 4. Variation of the voltage and the current at no load (phase s_{a1}).

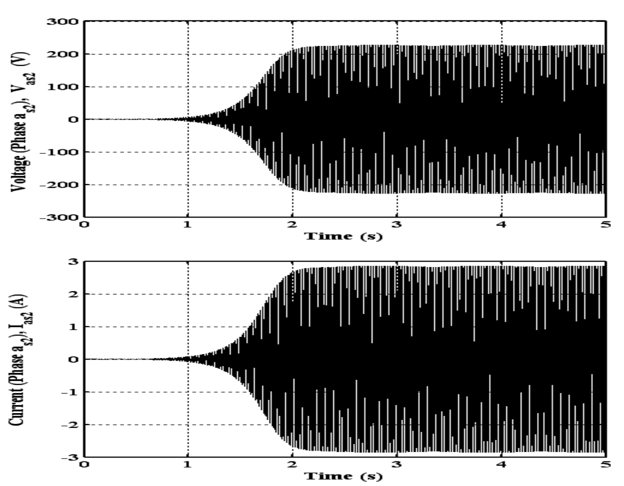

Fig. 5. Variation of the voltage and the current at no load (phase s_{a2}).

B. Excitation with Load

Figs. 7, 8, 10 and 11 show the variation of the voltage, current and the magnetizing current of the dual-stator windings of induction generator sets I and II respectively. At $t = 3s$, the three-phase star load are connected, in the first one, a purely resistive load of 200Ω is applied, the generated voltage, the stator current and the magnetizing current decrease respectively to 74.55%, 78.93% and 70.86% regarding to the values at no load. In the second one, a resistive-inductive load ($R = 200\Omega$ and $L = 0.05H$) is applied. In this case, the generated voltage, the stator current and the magnetizing current decrease respectively to 12.72%, 14.67% and 15.35%. Fig. 9 shows the variation of the load current at resistive load.

Application of the load, as the case of classical asynchronous generator, cause the decrease of the voltage generated by the decrease of the magnetizing current. Furthermore, the introduce of an inductive load generate more important decrease of reactive power.

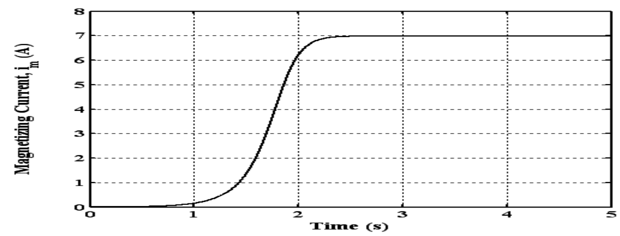

Fig. 6. Variation of the magnetizing current at no load.

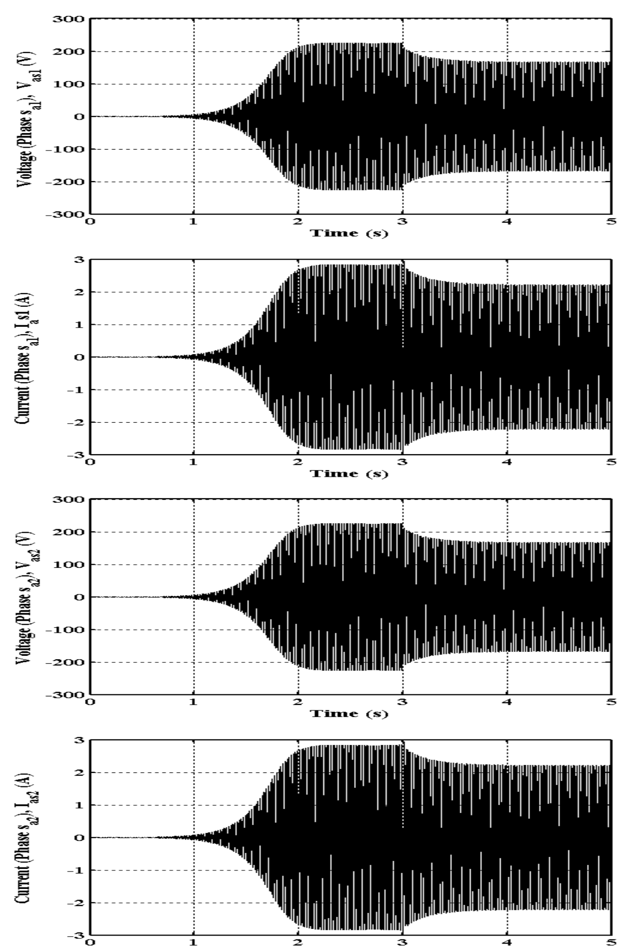

Fig. 7. Variation of the voltage and the current at resistive load.

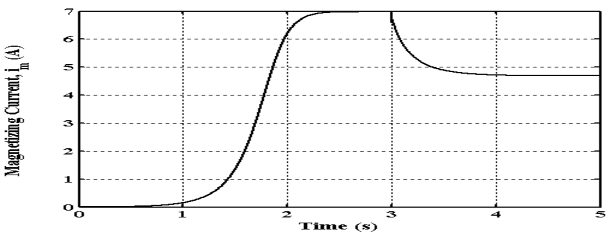

Fig. 8. Variation of the magnetizing current at resistive load.

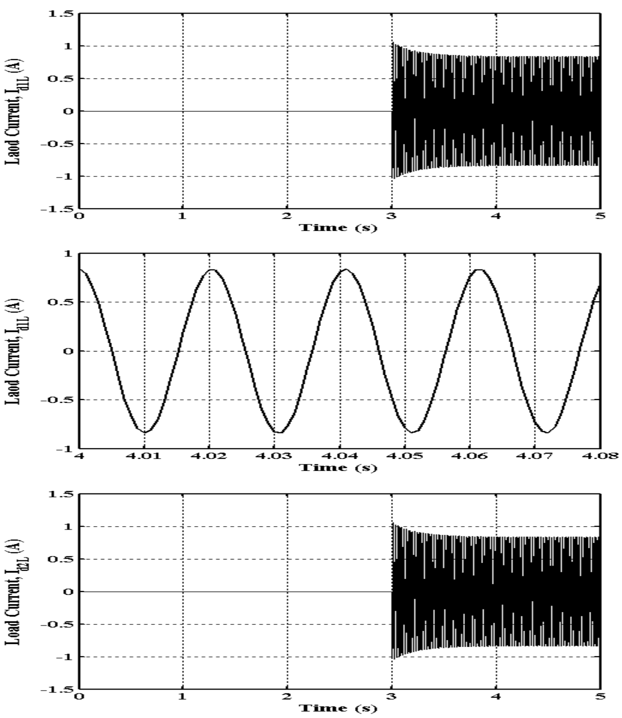

Fig. 9. Variation of the load current at resistive load.

IV. Conclusion

In this paper, a unified mathematical model for dual-stator winding induction generator has been developed, by including the common mutual leakage inductance between the two sets of stator winding. The simulation at no load and at load of this generator has been presented. The magnetizing inductance is the main factor for voltage build-up and stabilization of generated voltage for the different conditions.
The application of the load, as in the case of classical asynchronous generator, cause the decrease of the voltage generating by the decrease of the magnetizing current cause the decreasing of the reactive power.
Furthermore, in the purpose to perform the generator and his integrated in the wind system, we aim to apply a several control technics, such as : sliding mode and adaptive fuzzy logic control across static converters.

V. Appendix

The machine parameters used in the simulation are as follows [12]:

- Stator resistances per-phase (winding set I and II) $r_1 = r_2 = 1.9\Omega$;

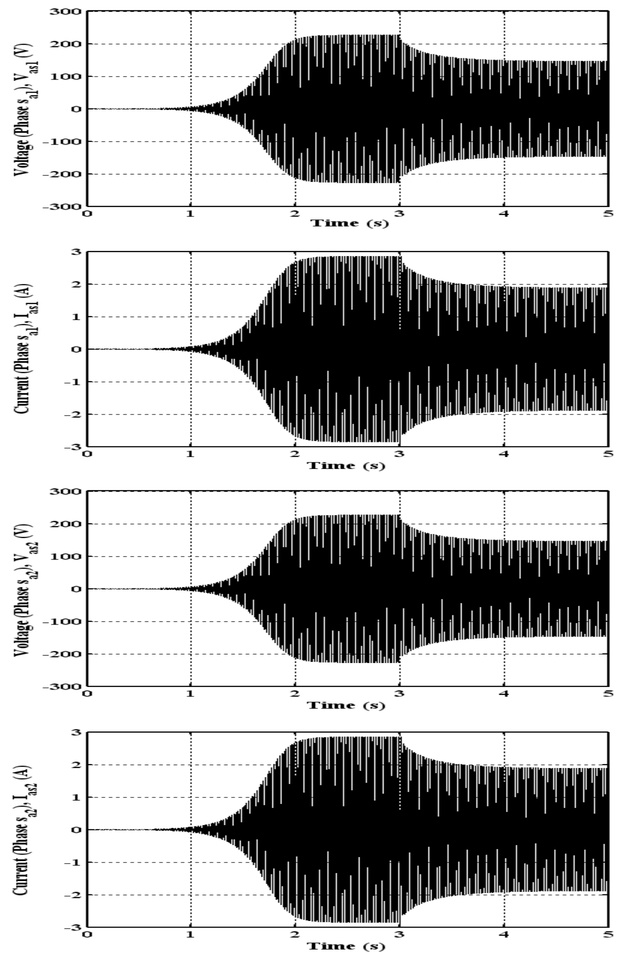

Fig. 10. Variation of the voltage and the current at resistive-inductive load.

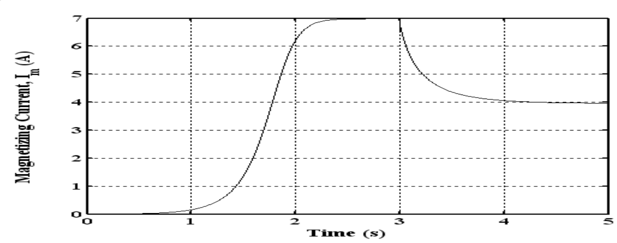

Fig. 11. Variation of the magnetizing current at resistive-inductive load.

- Stator leakage inductances per-phase (winding set I and II) $L_{l1} = L_{l2} = 0.0132H$;
- Rotor per-phase resistance $r_r = 2.1\Omega$;
- Rotor per-phase leakage inductance $L_{lr} = 0.0132H$;
- Common mutual leakage inductance $L_{lm} = 0.011H$;
- Moment of inertia $J = 0.038Kg.m^2$.

References

[1] B. Palle, M. G. Simões and F. A. Farret, “Dynamic simulation and analysis of parallel self-excited induction generator for islanded wind fram systems,” *IEEE Trans. Ind. Applicat.*, vol. 41, no. 4, pp. 1099–1106, July/Aug. 2005.

[2] F. A. Farret, B. Palle and M. G. Simões, “Full expandable model of parallel self-excited induction generators,” *IEE Proc.-Electr. Power Appl.*, vol. 152, no. 1, pp. 96–102, Jan. 2005.

[3] L. Wang and J. Y. Su, "Dynamic performances of an isolated self-excited induction generator under various loading conditions," *IEEE Trans. Energy Convers.*, vol. 14, no. 1, pp. 93–100, Mar. 1999.

[4] D. Hadiouche, H. Razik and A. Rezzoug, "On the modeling and design of dual-stator windings to minimize circulating harmonic currents for VSI fed AC machines," *IEEE Trans. Ind. Applicat.*, vol. 40, no. 2, pp. 506–515, Mar./Apr. 2004.

[5] R. Bojoi, A. Tenconi, G. Griva and F. Profumo, "Vector control of dual-three-phase induction-motor drives using two current sensors," *IEEE Trans. Ind. Applicat.*, vol. 42, no. 5, pp. 1284–1292, Sep./Oct. 2006.

[6] E. A. Klingshirn, "High phase order induction motors-Part I-description and theoretical considerations," *IEEE Trans. Power App. Syst.*, vol. PAS-102, no. 1, pp. 47–53, Jan. 1983.

[7] F. E. Sousy, M. Orabi and H. Godah, "Indirect field orientation control of self-excited induction generator for wind energy conversion system," *in 2004 IEEE International Conference on Industrial Technology (ICIT)*, pp. 480–485.

[8] D. Seyoum, C. Grantham and M. F. Rahman, "The dynamic characteristics of an isolated self-excited induction generator driven by a wind turbine," *IEEE Trans. Ind. Applicat.*, vol. 39, no. 4, pp. 936–944, July/Aug. 2003.

[9] N. H. Malik and A. H. Al-Bahrani, "Influence of the terminal capacitor on the performance characteristics of a self-excited induction generator," *IEE Proceedings*, vol. 137, Pt. C, no. 2, pp. 168–173, Mar. 1990.

[10] G. K. Singh, K. Nam and S. K. Lim, "A simple indirect field-oriented control scheme for multiphase induction machine," *IEEE Trans. Ind. Electron.*, vol. 52, no. 4, pp. 1177–1184, Aug. 2005.

[11] O. Ojo and I. E. Davidson, "PWM-VSI inverter-assisted stand-alone dual stator winding induction generator," *IEEE Trans. Ind. Applicat.*, vol. 36, no. 6, pp. 1604–1611, Nov./Dec. 2000.

[12] G. K. Singh, K. B. Yadav and R. P. Saini, "Modeling and analysis of multi-phase (six phase) self-excited induction generator," *In Proc. IEEE Conf. ICEMS'2005*, pp. 1922–1927, China, 2005.

[13] M. A. Ouhrouche, X. D. Do, Q. M. L and R. Chaine, "EMTP based simulation of a self-excited induction generator after its disconnection from the grid," *IEEE Trans. Energy Convers.*, vol. 13, no. 1, pp. 7–13, Mar. 1998.

[14] G. K. Singh, K. B. Yadav and R. P. Saini, "Analysis of a saturated multi-phase (six phase) self-excited induction generator," *International Journal of Emerging Electric Power Systems, The Berkeley Electronic Press*, vol. 7, no. 2, Article 5, pp. 1–21, 2006.

[15] D. Hadiouche, "Contribution to the study of dual stator induction machines : modeling, supplying and structure," (in french), Ph.D. dissertation, GREEN, Faculty Sci. Tech. Univ. Henri Poincar-Nancy I, Vandoeuvre-lès-Nancy, France, Dec. 2001.

[16] A. Kishore, R. C. Prassad and B. M. Karan, "Matlab simulink based dq modeling dynamic characteristics of three phase self-excited induction generator," *in Progress Electromagnetics Research Symposium*, Cambridge, USA, 26–29 Mar. 2006, pp. 312–316.

[17] S. K. Jain, J. D. Sharma and S. P. Singh, "Transient performance of three-phase self-excited induction generator during balanced and unbalanced faults," *IEE Proc.-Gener. Transm. Distrib.*, vol. 149, no. 1, pp. 50–57, Jan. 2002.

[18] K. E. Hallenius, P. Vas and J. E. Brown, "The analysis of a saturated self-excited asynchronous generator," *IEEE Trans. Energy Convers.*, vol. 6, no. 2, pp. 336–341, June 1991.

[19] Y. W. Liao and E. Levi, "Modeling and simulation of a stand-alone induction generator with rotor flux oriented control," *Electr. Power Syst. Res. 46*, pp. 141–152, 1998.

[20] A. Kishore and G. S. Kumar, "Dynamic modeling and analysis of three phase self-excited induction generator using generalized state-space approach," *in Internationnal Symposium on Power Electronics SPEEDAM 2006*, S15, pp. 52–59.

[21] B. Singh and L. B. Shilpakar, "Analysis of a novel solid state voltage regulator for a self-excited induction generator during balanced and unbalanced faults," *IEE Proc.-Gener. Transm. Distrib.*, vol. 145, no. 6, pp. 50–57, Nov. 1998.

[22] B. Singh, M. V. Verma and A. K. Tandon, "Rating reduction of static compensator for voltage control of three-phase self-excited induction generator," *in IEEE ISIE*, Montréal, Québec, Canada, Jul. 9–12, 2006, pp. 1194–1199.

[23] T. Ahmed, K. Nishida and H. W. Lee, "Self-excited induction generator with simple voltage regulation scheme for wind turbine," *in The 30th Annual Conf. IEEE Ind. Electron. Society*, Bussan, Korea, Nov. 2–6, 2004, pp. 86–91.

Hocine Amimeur was born in Bejaia, Algeria. He received the Electrical Engineer degree from the University of Bejaia, Algeria, in 2005.

He then joined the Department of Electrical Engineering of the University of Batna. His research interests include analysis and modeling of dual-stator windings induction generators, simulation and control of dual-stator windings induction machines, and renewable energy.

Rachid Abdessemed was born in Batna, Algeria, in 1951. He received the M.Sc. and Ph.D. degrees in Electrical Engineering from Kiev Polytechnic Institute, Kiev, Ukraine, in 1978 and 1982, respectively.

He has been working for more than 19 years with the Department of Electrical Engineering, University of Batna, as a Professor. Currently, he is the Director of the Electrical Engineering Laboratory. His current area of research includes design and control of induction machines, reliability, magnetic bearing, and renewable energy.

Djamal Aouzellag received the Bachelor of Science in Maintenance of the Electrical Appliance of Plane and the Systems of Navigation in 1993, the Master in Electrical Engineering in 1995 from Aeronautics Institute of Riga - Latvia and the PhD in System and Processes Controls in 2001 from National University of Aeronautics, Kiev - Ukraine. Currently, he is Instructor at the University of Bejaa, Algeria. His Research interests include the Renewable Energy and the Electric Drive.

Elkheir Merabet was born in Bordj-Bou-Arréridj, Algeria, in 1982. He received the Electrical Engineer degree from the University of M'sila, Algeria, in 2005.

He then joined the Department of Electrical Engineering of the University of Batna. His research interests include analysis and modeling of dual-stator windings induction generators, simulation and control of dual-stator windings induction machines, and renewable energy.

Farid Hamoudi was born in Bejaia, Algeria. He received the Electrical Engineer degree from the University of Bejaia, Algeria, in 2005.

He then joined the Department of Electrical Engineering of the University of Batna. His main subjects of research concern electrical machines, diagnostics, control, power systems and renewable energy.